ORIGINAL RESEARCH

Smoking Exposure Induces Human Lung Endothelial Cell Adaptation to Apoptotic Stress

Daniela N. Petrusca[1], Mary Van Demark[1], Yuan Gu[1], Matthew J. Justice[1], Adriana Rogozea[1], Walter C. Hubbard[3], and Irina Petrache[1,2]

[1]Department of Medicine, Division of Pulmonary, Allergy, Critical Care, and Occupational Medicine, Indiana University School of Medicine, Indianapolis, Indiana; [2]Richard L. Roudebush Veteran Affairs Medical Center, Indianapolis, Indiana; and [3]Department of Pharmacology, Johns Hopkins University, Baltimore, Maryland

Abstract

Prolonged exposure to cigarette smoking is the main risk factor for emphysema, a component of chronic obstructive pulmonary diseases (COPDs) characterized by destruction of alveolar walls. Moreover, smoking is associated with pulmonary artery remodeling and pulmonary hypertension, even in the absence of COPD, through as yet unexplained mechanisms. In murine models, elevations of intra- and paracellular ceramides in response to smoking have been implicated in the induction of lung endothelial cell apoptosis, but the role of ceramides in human cell counterparts is yet unknown. We modeled paracrine increases (outside-in) of palmitoyl ceramide (Cer16) in primary human lung microvascular cells. In naive cells, isolated from nonsmokers, Cer16 significantly reduced cellular proliferation and induced caspase-independent apoptosis via mitochondrial membrane depolarization, apoptosis-inducing factor translocation, and poly(ADP-ribose) polymerase cleavage. In these cells, caspase-3 was inhibited by ceramide-induced Akt phosphorylation, and by the induction of autophagic microtubule-associated protein-1 light-chain 3 lipidation. In contrast, cells isolated from smokers exhibited increased baseline proliferative features associated with lack of $p16^{INK4a}$ expression and Akt hyperphosphorylation. These cells were resistant to Cer16-induced apoptosis, despite presence of both endoplasmic reticulum stress response and mitochondrial membrane depolarization. In cells from smokers, the prominent up-regulation of Akt pathways inhibited ceramide-triggered apoptosis, and was associated with elevated sphingosine and high-mobility group box 1, skewing the cell's response toward autophagy and survival. In conclusion, the cell responses to ceramide are modulated by an intricate cross-talk between Akt signaling and sphingolipid metabolites, and profoundly modified by previous cigarette smoke exposure, which selects for an apoptosis-resistant phenotype.

Keywords: sphingolipids; chronic obstructive pulmonary disease; apoptosis; autophagy; high-mobility group box 1

Clinical Relevance

The main finding that chronic exposure to cigarette smoking changes the phenotype of human lung microvascular endothelial cells, selecting for an apoptosis-resistant and more proliferative population, may be relevant to the pathogenesis of chronic obstructive pulmonary disease (COPD). This hyperproliferative phenotype resembles that of endothelial cells isolated from lesions of idiopathic arterial pulmonary hypertension. Whereas lung microvascular endothelial cell apoptosis has been implicated in the initiation and progression of emphysema, the adaptation to apoptosis or surviving cells may contribute to the development of pulmonary vascular remodeling in COPD.

Cigarette smoke (CS) exposure is one of the main risk factors of chronic obstructive pulmonary disease (COPD), a syndrome with many phenotypes, including emphysema. The latter is characterized by increased apoptosis of cells comprising the alveolar wall. This destructive process particularly targets lung microvascular endothelial cells and alveolar epithelial cells,

(Received in original form January 16, 2013; accepted in final form September 19, 2013)

This work was supported by RO1HL077328, Reba and Floyd Smith Chair in Respiratory Disease, Calvin English Chair (I.P.) and T35 HL007802 (D.K. Ndishabandi).

Correspondence and requests for reprints should be addressed to Daniela N. Petrusca, Ph.D., Indiana University, Division of Pulmonary, Allergy, Critical Care and Occupational Medicine, Walther Hall-R3 C446, 980 West Walnut Street, Indianapolis, IN 46202-5120. E-mail: dpetrusc@iupui.edu

This article has an online supplement, which is accessible from this issue's table of contents at www.atsjournals.org

Am J Respir Cell Mol Biol Vol 50, Iss 3, pp 513–525, Mar 2014

Originally Published in Press as DOI: 10.1165/rcmb.2013-0023OC on September 30, 2013
Internet address: www.atsjournals.org

as noted in human lung samples or animal models of disease (1). Previous work in murine models indicated that endothelial and epithelial cell apoptosis leading to emphysema is due to up-regulation of ceramides, sphingolipid species with pleiotropic biological actions (2–5). Furthermore, lungs of human subjects with emphysema or even smokers that have not yet developed the disease exhibit increased lung ceramide levels (2, 6), together with increased apoptosis and autophagy (7–10). Although these findings implicate ceramide elevations in the lungs of smokers as potential triggers or mediators of endothelial cell apoptosis, this hypothesis has not yet been tested in human cells. In addition, it is not known if endothelial cells challenged with ceramide transition through autophagy before undergoing apoptosis.

Autophagy, a mechanism of cellular constituent recycling, can be triggered during endoplasmic reticulum (ER) stress (11) or by increases in the danger-associated signaling molecule high-mobility group box 1 (HMGB1) (12), as an attempt to maintain cell survival. Depending on the cell's adaptive or repair capacity, autophagy may be followed by apoptosis. However, the key molecular events that determine the switch from autophagy to survival or apoptosis during exposure to CS in general, or to ceramides in particular, are not known. This is of particular importance, as aberrant lung endothelial cell responses may contribute to pulmonary vascular remodeling frequently observed in COPD. A better understanding of the effects of ceramide on human lung endothelial cell survival, autophagy, and apoptosis parameters is therefore needed.

We investigated the response of primary human lung microvascular endothelial cells (LMVECs) to long-chain palmitoyl ceramide (Cer16), because this is one of the most abundant lung ceramides (6), which is associated with lung endothelial cell apoptosis *in vivo* and *in vitro* (13). Cells exposed to exogenous ceramide trigger further endogenous ceramide production via the *de novo* synthesis pathway (14), which requires the action of the dihydroceramide (DHC) desaturase on DHC, the immediate precursor of ceramide. DHC is itself an active metabolite with antiproliferative activities (15). Through the action of ceramidases, endogenous ceramides can be further metabolized to sphingosine (SPH) and SPH 1-phosphate (S1P). Although S1P has well characterized prosurvival functions, the effect of SPH during cellular adaptation to stress is not known.

We demonstrate that primary human lung endothelial cell responses to Cer16 are profoundly modulated by previous CS exposure, and that, unlike murine cells, their survival responses are very robust. As expected, C16 ceramide induced apoptosis in naive endothelial cells. However, chronic *in vivo* CS exposure may lead to the selection of an apoptosis-resistant, proliferating cell population that exhibits up-regulation of prosurvival and stress-response pathways, such as Akt and HMGB1.

Materials and Methods

Materials

Ceramides with short (Cer6:0) or intermediate (Cer16) fatty acid chain and polyethylene glycol–conjugated ceramide Cer16-PEG 2,000 were purchased from Avanti Polar Lipids (Alabaster, AL). The inhibitors used were from Sigma-Aldrich (St. Louis, MO), with the exception of: ZVAD-fmk (MBL, Woburn, MA); (1*S*,2*R*)-D-erythro-2-(*N*-myristoylamino)-1-phenyl-1-propanol (Biomol Int., Plymouth Meeting, PA), and LY294002 (Calbiochem, San Diego, CA). All antibodies were purchased from Cell Signaling unless otherwise stated.

Cells

LMVECs from smoker and nonsmoker donors (Lonza, Walkersville, MD) and human small airway epithelial cells (Lonza) were maintained in complete culture medium consisting of microvascular endothelial cell growth medium and small airway epithelial cell growth medium, respectively, supplemented with their specific SingleQuots (Lonza). The smoking status of the donor was provided by the cell supplier (Lonza).

Viability/Proliferation Assay

The assay was performed by using an *in vitro* 3-(4,5-dimethylthiazol-2-yl)-2,5-diphenyl tetrazolium bromide (MTT) assay (Sigma-Aldrich), as previously described. The absorbance of formazan was measured at 570 nm.

Apoptosis

Apoptosis was quantified by annexin V/propidium iodide staining using an apoptosis detection kit (R&D Systems, Minneapolis, MN) and flow cytometry using a Cytomics FC500 cytofluorimeter with CXP software (Beckman Coulter, Fullerton, CA).

Caspase Activity Assay

Caspase-3 activity was determined with Apo-ONE Homogeneous Caspase-3/7 Assay (Promega, Madison, WI) using a SpectraMax M2 plate reader (Molecular Devices Inc., Sunnyvale, CA).

Mitochondrial Depolarization

Mitochondrial depolarization was measured with the MitoCaptureApoptosis Detection Kit (Calbiochem). Its main reagent is a cationic dye that accumulates in healthy mitochondria in aggregates that fluoresce in red. Any stimuli that alter the mitochondrial membrane potential maintain the dye in its monomeric form, that fluoresces in green. As positive control, cells were treated with staurosporine (0.2 μM, 2 h), and quantification was done by flow cytometry.

Cell Fractionation

Cell fractionation was achieved with Mitochondria/cytosol and Nuclear/cytosol fractionation kits (BioVision, Mountain View, CA), according to the manufacturer's protocol.

Western Blotting

Equal protein amounts, as determined by bicinchoninic acid assay protein analysis (Pierce, Rockford, IL), were separated by SDS-PAGE and transferred onto a polyvinylidene difluoride membrane, followed by routine immunoblotting (16). Immune complexes were detected using enhanced chemiluminescence (Amersham Biosciences, Buckinghamshire, UK), quantified by densitometry and normalized using specific loading controls.

Sphingolipids Determination

Lipid extraction and total lipid phosphorus measurements were performed as previously described (2).

Efferocytosis Assay

LMVECs were stained with Cell Tracker Green (Invitrogen, Carlsbad, CA) and treated with apoptosis inducers for 6 hours

followed by coculture (5:1) with rat macrophages for 1 hour. Efferocytosis was quantified by flow cytometry (6), and results were expressed as efferocytosis index (number of macrophages that engulfed apoptotic cells × 100).

Electron Microscopy

Samples were analyzed on a Tecnai G2 12 Bio Twin transmission electron microscope (FEI, Hillsboro, OR) equipped with a charge-coupled device camera (Advanced Microscopy Techniques, Danvers, MA).

Immunocytofluorescence

Cells were stained with Mitotracker Red CMXRos (Molecular Probes/Invitrogen), fixed with paraformaldehyde (4%), and permeabilized with 0.2% Triton X-100 in PBS. Cells were then incubated with apoptosis-inducing factor (AIF) antibody (AbCam, Cambridge, MA), followed by FITC-labeled goat anti-rabbit IgG (AbCam). Images were obtained using an Eclipse 80I fluorescence microscope with camera and NIS-Elements AR 3.0 15 software (Nikon, Melville, NY).

Statistical Analysis

Statistical analysis was performed using SigmaStat 3.5 (San Jose, CA). Differences between groups were compared using unpaired Student's *t* test. All experiments were done at least three times, and the data were expressed as means (± SEM). Statistical difference was accepted at a *P* value less than 0.05.

Results

Effects of Cer16 on Human LMVEC Proliferation

Human primary LMVECs were obtained from donors with a history of either never-smoking (nonsmoker donor; also named naive cells) or with a history of previous CS exposure (smoker donor). Demographic and brief clinical characteristics of the donors are listed in Table E1 in the online supplement. Interestingly, the baseline MTT activity of cells from smoker donors was noted to be 1.6-fold higher than that of cells from nonsmokers (Figure 1a). This baseline proliferative activity was associated with marked divergent expression or cell cycle control proteins. In particular, $p16^{INK4a}$ (inhibitor of CDK4 family) was reduced and retinoblastoma protein was hyperphosphorylated in LMVECs from smokers compared with naive cells (Figure E1), further suggesting that cells from smoker donors have increased proliferation rates compared with those from nonsmokers.

When challenged with ceramide Cer16 and compared with vehicle control, human LMVECs exhibited marked, dose-dependent (Figure 1b), and sustained (Figure 1c) decreases in cell proliferation, regardless of the smoking status of the donor. Concentrations of ceramide that typically induce apoptosis in murine cultured cells or cell lines (10 μM and higher) significantly reduced LMVEC proliferative activity up to 50%, even as early as 2 hours after treatment (Figure 1c). We next evaluated whether ceramide reduced cell survival.

Human LMVEC Apoptotic and Survival Responses to Cer16

Ceramide Cer16 treatment (10 μM, 6 h) caused externalization of phosphatidylserine on LMVECs from nonsmokers, but not on those from smokers (Figure 2a). Neither higher concentrations, nor prolonged exposures to Cer16 (up to 20 μM for up to 24 h; data not shown) or shorter chain (Cer6) ceramide (Figure 2a) increased apoptotic annexin V staining in endothelial cells from smoker donors. Interestingly, the smoking-dependent effect of ceramide on apoptosis was cell type–specific, because both Cer16 and Cer6 significantly increased apoptosis in primary small airway epithelial cells from smoker donors, but not in those from nonsmoking donors (Figure 2b). As a complementary functional assay of phosphatidylserine externalization, we assessed whether ceramide-treated endothelial cells are engulfed (efferocytosed) by healthy (nontreated) macrophages. Fluorescently labeled LMVECs from smoker or nonsmoker donors were treated with TNF-α plus cycloheximide for 6 hours, a treatment known to induce endothelial cell apoptosis via endogenous ceramide signaling (14), or with Cer16. After treatment, endothelial cells were incubated in a phagocytosis assay with primary alveolar macrophages. As expected, there was a marked increase in macrophage-engulfed LMVECs treated with TNF-α plus cycloheximide, indicating that they underwent apoptosis, compared with control LMVECs (which were not apoptotic). Consistent with annexin V data, the number of engulfed endothelial cells from smokers that were treated with Cer16 was negligible and significantly lower than the number of engulfed Cer16-treated naive endothelial cells (Figure E3a). Indeed, macrophages engulfed only ceramide-treated LMVECs from nonsmokers. Therefore, surprisingly, measurements of the executioner caspase activity in human LMVECs from nonsmokers demonstrated early (2–6 h) inhibition of caspase-3/7 activity in response to Cer16 treatment, followed by a return to baseline levels (Figure 2c). In a distinct fashion, ceramide-treatment of LMVECs from smoker donors briskly (2 h) and only modestly activated caspase-3/7, which then remained inhibited (Figure 2c).

Together, these results suggest that Cer16 markedly decreases LMVEC proliferation, inducing apoptosis in a smoking status–dependent fashion. Therefore, we investigated if ceramide activated survival signaling pathways, such as extracellular signal–regulated kinase (ERK) 1/2 mitogen-activated protein kinase or Akt, as these promitogenic, antiapoptotic pathways can be engaged by ceramide in rat lung endothelial cells (16) or in lung macrophages (17), respectively. Ceramide modestly and transiently activated ERK1/2 in LMVECs from smokers at 6 hours (Figure 2 d, *upper panel*, Western blot and densitometry). In contrast, Akt activation was rapidly and significantly (at 6 h) induced by ceramide in naive LMVECs (Figure 2e, *upper panel*, Western blot, and *lower panel*, densitometry). Cells from smokers exhibited striking levels of Akt hyperphosphorylation even before ceramide treatment (Figure E4a), and ceramide had little additive effect during the studied timeframe (Figure 2e).

To determine the impact of survival pathway activation on cell proliferation and apoptosis, LMVECs were pretreated with PD98059 and LY29400, specific pharmacological inhibitors of ERK1/2 and Akt, respectively. Both inhibitors decreased cellular proliferation of unchallenged LMVECs (Figure E2). Inhibition of ERK1/2 (Figure 2 d, *lower panel*) further reduced cell proliferation in ceramide-treated cells from smokers (Figure E2a), but did not facilitate apoptosis (Figure 2f). In contrast, inhibition of Akt decreased the proliferation of ceramide-treated naive cells

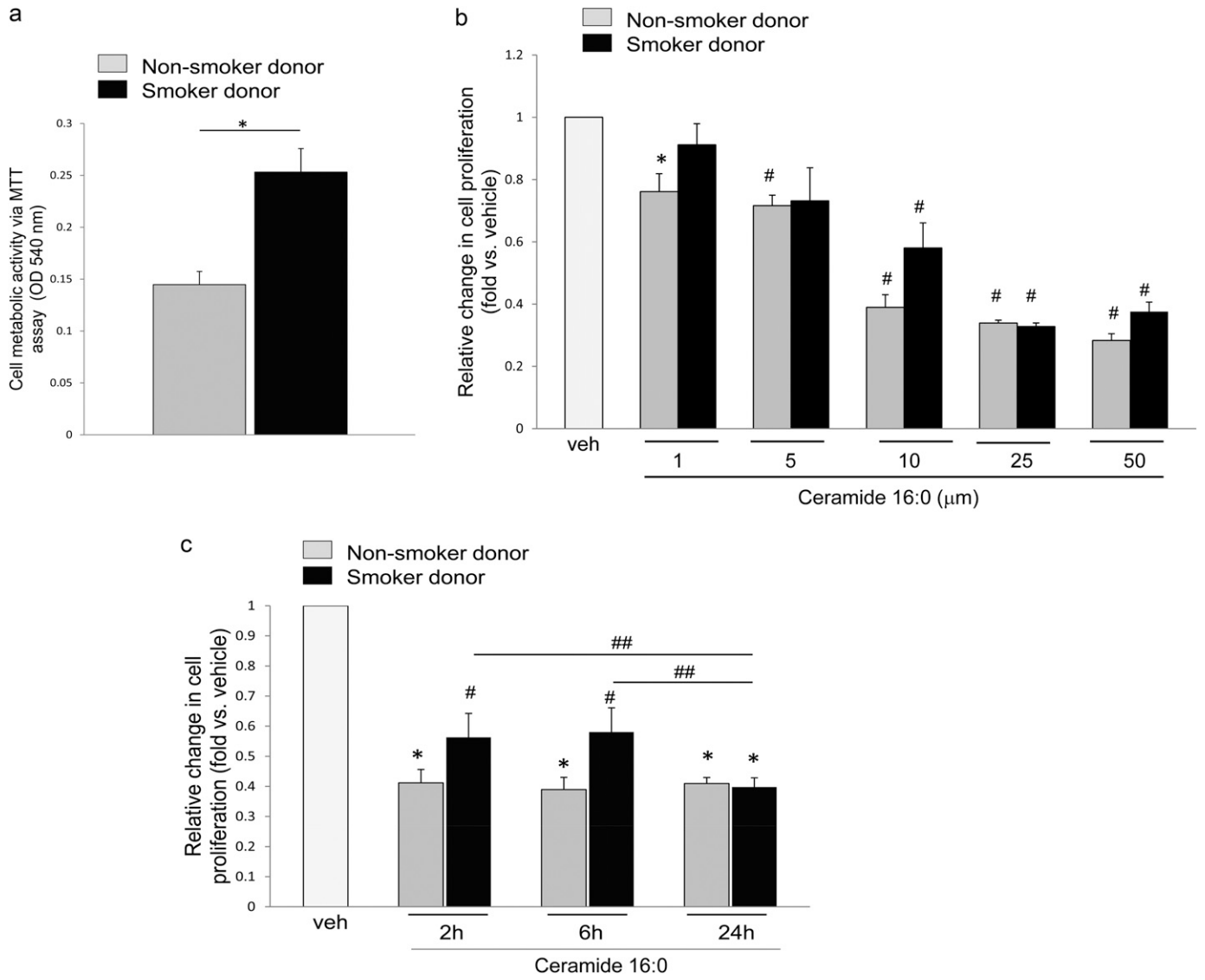

Figure 1. Inhibitory effects of palmitoyl ceramide (ceramide 16:0 [Cer16]) on the metabolic/proliferative activity of human lung microvascular endothelial cells. Metabolic activity measured by 3-(4,5-dimethylthiazol-2-yl)-2,5-diphenyl tetrazolium bromide (MTT) assay in cells from nonsmoker (*gray bars*) and smoker (*black bars*) in the following conditions: (*a*) untreated, 16 hours, mean + SEM ($n = 3$; $^{*}P < 0.05$); (*b*) following vehicle (veh; polyethylene glycol 2,000) or Cer16 treatment at the indicated concentrations (6 h), fold change versus veh, mean + SEM ($n = 3$; $^{*}P < 0.05$, $^{\#}P < 0.005$ vs. veh); or (*c*) following veh, or Cer16 treatment for the indicated time in hours (10 μM), mean + SEM ($n = 3$; $^{*}P < 0.0001$ and $^{\#}P < 0.01$ vs. vehicle control; $^{\#\#}P < 0.05$).

only (Figure E2b), while doubling their apoptosis levels (Figure 2f). These results indicate that LMVECs require ERK1/2 and Akt activity for basal levels of cell proliferation, regardless of smoking exposure, and that, in naive LMVECs, ceramide-induced Akt protects against apoptosis, with little contribution from ERK1/2. Moreover, inhibition of ERK had no effect on Akt activation (Figure E4b), inhibition of Akt stimulated ERK phosphorylation (Figure E4c), suggesting an interactive, compensatory prosurvival signaling.

To investigate whether a caspase-independent mechanism contributes to ceramide-induced apoptosis in LMVECs, we focused on mitochondria. Ceramide treatment rapidly and markedly altered the mitochondrial membrane potential in LMVECs from nonsmokers (Figure 3a). In agreement with the lack of executioner caspase activation in these cells, the mitochondrial depolarization occurred in a caspase-independent manner, because a general caspase inhibitor, ZVAD-fmk, did not prevent ceramide-induced mitochondrial membrane depolarization (Figure E3b). LMVECs from smoker donors depolarized mitochondria in a caspase-independent fashion as well (Figure E3c), albeit to a lesser degree, compared with cells from nonsmokers (Figure 3a). In both cell types, but especially in smokers' cells, Akt had an inhibitory role on mitochondrial membrane depolarization (Figure 3a). Cer16 treatment of naive LMVECs, but not those from smokers, caused AIF translocation from the mitochondria to the nucleus, as detected by Western blotting of cell fractions (Figure 3b) and by immunofluorescence

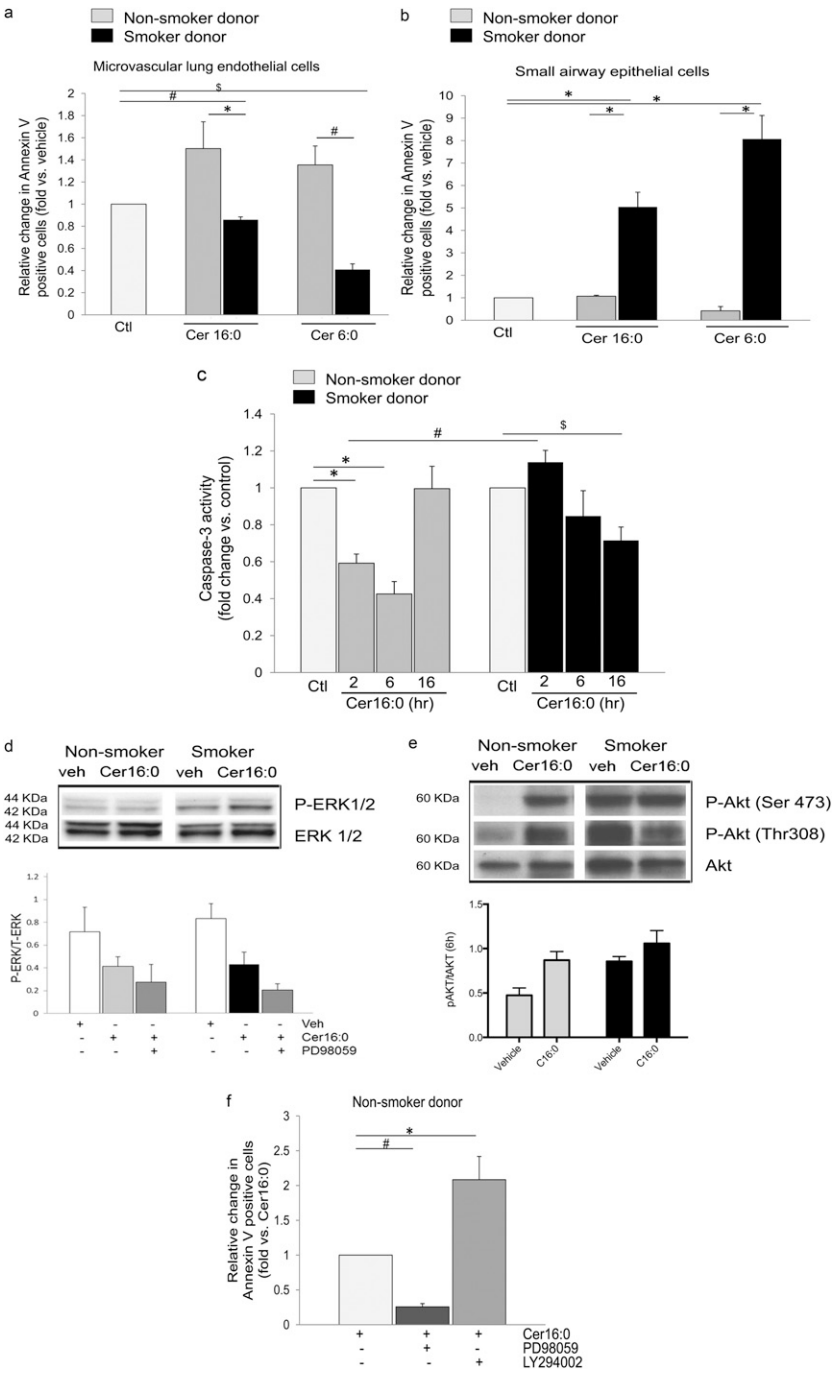

Figure 2. Apoptosis and survival responses of human lung microvascular endothelial cells to Cer16. (*a* and *b*) Apoptosis measured by annexin V/propidium iodide staining and expressed as fold increase in positive cells versus control vehicle in human lung microvascular endothelial cells (*a*) compared with human small airway epithelial cells (*b*), both isolated from either nonsmokers (*gray bars*) or smokers (*black bars*). Cells were treated with Cer16 or Cer6 (10 μM; 6 h), or with vehicle (PEG 2,000); mean + SEM (n = 4; $^{*}P < 0.05$, $^{\#}P = 0.006$, and $^{\$}P < 0.001$). (*c*) Caspase-3 activity of human lung microvascular endothelial cells treated Cer16 (10 μM) or vehicle (control [Ctl]) for the indicated time. Mean + SEM. (n = 9; $^{*}P < 0.05$, $^{\#}P = 0.006$, and $^{\$}P = 0.05$. (*d*) Activated and total extracellular signal–regulated kinase (ERK) 1/2 measured by Western blot in lung microvascular endothelial cells (LMVECs) lysates from nonsmoker and smoker donors after treatment with Cer16 (10 μM) or vehicle (veh) for 6 hours (*upper panel*, Western blot) and 16 hours (*lower panel*, densitometry). Mean + SEM; n = 4. (*e*) Activated and total Akt in LMVEC lysates treated with either Cer16 (10 μM) or vehicle for 6 hours (*upper panel* showing Western blot and *lower panel* showing densitometry). Mean + SEM (n = 4; two-way ANOVA showing $P < 0.05$ for both Cer treatment and smoking status). (*f*) Effect of ERK1/2 or Akt inhibition on LMVEC apoptosis measured by annexin V/PI staining in cells from nonsmoker donors. Cells were pretreated (1 h) with either PD98059 (10 μM) or LY294002 (30 μM) followed by Cer16 (10 μM, 2 h). Results are expressed as fold change versus Cer16. Mean + SEM (n = 3; $^{*}P = 0.01$, $^{\#}P < 0.0001$). P-Akt, phosphorilated serine/threonine-specific protein kinase; P-ERK, phosphorilated extracellular signal–regulated kinase; Ser, serine; Thr, threonine.

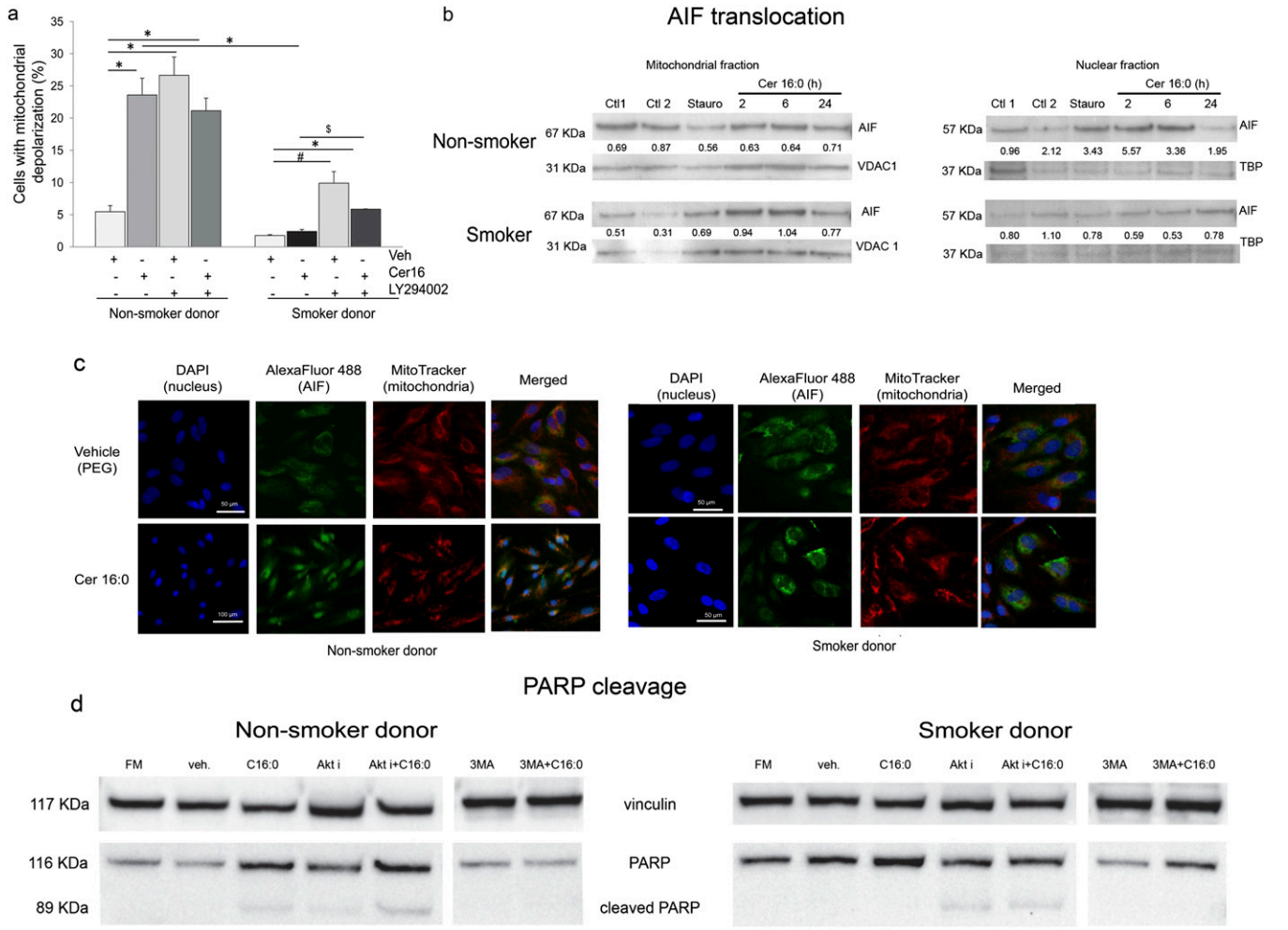

Figure 3. Mitochondria changes in human lung microvascular endothelial cells treated with Cer16. (*a*) Mitochondria depolarization in cells treated with Cer16 (10 μM, 6 h) or vehicle (Veh) and effect of Akt inhibitor LY294002 (30 μM, 1 h pretreatment). Mean + SEM ($n = 3$; $^{*}P < 0.05$, $^{\#}P < 0.001$, $^{\$}P = 0.05$). (*b* and *c*) Apoptosis-inducing factor (AIF) translocation from mitochondria to nucleus detected by Western blot (*b*) in respective cellular subfractions of cells treated with Cer16 (10 μM; for the indicated time in hours) or its Veh (PEG 2000; Ctl1) compared with staurosporine (Stauro; 0.2 μM, 2 h) or its Veh (Ctl2). Loading controls for each subcellular fraction, voltage-dependent anion channel (VDAC1) and TATA-binding protein (TBP), were detected in the *lower lanes*. Densitometry of AIF expression normalized by loading control is indicated numerically in between lanes. (*c*) Representative fluorescence micrographs of cells immunostained for AIF (FITC-labeled). Mitochondria are stained in *red* (MitoTracker Red) and nuclei in *blue* with 4′,6-diamidino-2-phenylindole (DAPI) after treatment with Cer16 (10 μM) or Veh; *scale bar*, 50 μm. (*d*) Detection of cleaved poly(ADP-ribose) polymerase (PARP) in total protein lysates of cells: untreated, grown in regular full serum–containing media (FM); or treated with Veh or Cer16 (10 μM, 6 h), and either Akt inhibitor (30 μM LY294002; 1 h pretreatment) or autophagy inhibitor, 3-methyladenine (3-MA; 5 mM, 1 h pretreatment). Vinculin expression was used as loading control.

(Figure 3c). Consistent with AIF translocation, ceramide treatment cleaved poly(ADP-ribose) polymerase (PARP) only in LMVECs from nonsmokers (Figure 3d). In contrast, in LMVECs from smokers, ceramide-induced PARP cleavage was noted only in the presence of Akt inhibitor (Figure 3d). These results suggest that ceramide induces caspase-independent mitochondrial activation, AIF translocation, and PARP cleavage apoptosis in LMVECs from nonsmokers. In contrast, LMVECs from smokers are more resistant to ceramide-induced apoptosis, in large part via Akt activation.

Human LMVEC Autophagy in Response to Cer16

The conversion via lipidation of microtubule-associated protein 1 light-chain 3 (LC3) from LC3-I (free form) to LC3-II (membrane-bound form) is a key step in the induction of autophagy in mammalian cells. Primary human LMVECs displayed basal levels of LC3-II expression in culture conditions of low serum–containing media (Figure 4a). The conversion of LC3-I to LC3-II was increased by Cer16, regardless of the smoking status of the donor (Figure 4a). This effect was noted as early as 6 hours after ceramide treatment (Figure 4b), and persisted for 16 hours (Figures 4a and 4b). The autophagy inhibitor 3-methyladenine (3-MA), although not affecting LC3-II levels in untreated cells, inhibited ceramide-induced LC3-I to LC3-II conversion (Figure 4a). Treatment with ZVAD-fmk did

not alter ceramide-induced autophagy (Figures 4a and E5e). Autophagy was confirmed by electron microscopy, which showed an increased number of autophagosomes after ceramide treatment (Figure 4b), without impairment of the autophagic flux (Figures E5a–E5c). Electron microscopy images of ceramide-induced autophagy unveiled concomitant ER stress, characterized by swelling of the ER lumen (Figure 4b). Ceramide-induced ER stress was confirmed biochemically by Western blotting for phospho- and total eukaryotic translation initiation factor 2a (eIF2α). Ceramide treatment increased eIF2α phosphorylation in all LMVECs (Figures 4c and E4d). Inhibition of autophagosome formation with 3-MA modestly increased phospho-eIF2α levels in ceramide-treated cells, suggesting that autophagy may partly attenuate ER stress (Figures 4c and E4d). The effect of caspase inhibition on ER stress was equivocal, having no effect in ceramide-treated naive LMVECs, while enhancing it in LMVECs from smokers (Figure 4c).

Interestingly, only in naive LMVECs, inhibition of autophagy with 3-MA protected against mitochondrial depolarization (Figure 5b) and PARP cleavage (Figure 3d), while inducing caspase-3 activation (Figure 5a), indicating that induction of autophagy is a prerequisite for caspase-3–independent apoptosis of these cells, and that its inactivation compels the cells into caspase-3–dependent apoptosis.

To further understand the complex interrelationship between autophagy and apoptosis, we investigated the involvement of HMGB1, a danger-associated molecular pattern and ligand of the receptor for advanced glycation end products found to be elevated in the blood, bronchoalveolar lavage fluid, and lung tissue of patients with COPD (18 and 19). HMGB1 involvement in autophagy (20) and apoptosis (21, 22) has been recently described. Moreover, its intracellular overexpression was recently correlated with angiogenesis (23) and proliferation (24). Because LMVECs from smokers exhibited enhanced autophagy rather than apoptosis in response to ceramide treatment and were more proliferative at baseline, we investigated if prosurvival pathways modulated HMGB1 levels in these cells. HMGB1 was noticeably increased in LMVECs from smokers compared with nonsmokers (Figures 5c and E4f). Ceramide treatment increased HMGB1 at 6 hours (Figures 5c and E4f). Neither protein synthesis inhibition, nor ERK1/2 inhibition altered HMGB1 expression (Figure 5c). Similarly, HMGB1 levels were not affected by caspase inhibitors or 3-MA (data not shown). Instead, HMGB1 expression in cells from smokers, both at baseline and in response to ceramide, was dependent on Akt phosphorylation, because Akt inhibition markedly reduced HMGB1 levels, concomitant with diminishing LC3 lipidation (Figure 5c). These data suggest the involvement of HMGB1 in the apoptosis-resistant phenotype induced by chronic smoking.

Involvement of Endogenous Sphingolipids in LMVEC Autophagy

Exogenously administered ceramide is known to exert biological effects in large part due to stimulation of endogenous ceramides synthesis. The effect of outside-in ceramides on other metabolites that may impact cell proliferation and survival, such as DHCs, SPH, or S1P, is not well described. We determined sphingolipid levels in LMVECs by tandem mass spectrometry. As expected, Cer16 treatment markedly elevated total ceramides in LMVECs (Figure 6a), accompanied by significant, albeit less robust, increases in DHC (Figure 6b). The DHC content in cells from nonsmokers was under the control of Akt, as Akt inhibition markedly increased DHC levels in these cells, with negligible effect of ceramide levels, suggesting that Akt activity may be linked to DHC desaturase activity, which converts DHC to ceramide.

Cer16 also elevated downstream production of SPH levels in cells from smokers, which already had elevated SPH levels, but not in naive cells (Figure 6c). The increase in SPH, which indicates activation of ceramidases, was also influenced by Akt activity. Interestingly, SPH levels were modified by treatment with the autophagy inhibitor, 3-MA, in all cells (Figure 6c). Although Cer16 up-regulated SPH, this was not translated into increased S1P levels; rather, ceramide-treated cells had less S1P content, indicating concomitant lack of activation or even inhibition of SPH kinases (Figure 6d). It was surprising that LMVECs from smokers had reduced S1P levels compared with those from nonsmokers (Figure 6d), given their propensity for increased survival (Figure 6e). To further explore the significance of SPH production, we used the ceramidase inhibitor, (1*S*,2*R*)-D-erythro-2-(*N*-myristoylamino)-1-phenyl-1-propanol, and measured the MTT activity of LMVECs. Inhibition of ceramidase diminished MTT activity in untreated and ceramide-treated LMVECs (Figure 6e), reduced HMGB1 levels, and reduced LC3 lipidation (Figure 6f), indicating that SPH may contribute to the prosurvival adaptation of LMVECs.

Discussion

The synthesis of ceramide species at the plasma membrane increases their paracellular bioavailability where they exert paracrine and/or autocrine effects. Our results show that lung endothelial cellular responses to a ceramide-rich milieu include a general decrease of cell metabolism and proliferation, and induction of autophagy with or without apoptosis, depending on the smoking exposure history of the donor (Figure 7). These findings may relate to the pathogenesis of emphysema, a disease typically associated with intermittent, but chronic, exposure to cigarette smoking, which increases both intra- and paracellular ceramides. The fact that ceramide induced the expression of ER stress response markers and the up-regulation of HMGB1 and Akt pathways, which are both detected in human COPD lungs, indicates potential relevance of our findings to human disease. Because active challenges of human lung structural cells cannot be performed *in vivo*, we have employed a reductionist approach to directly assess responses to extracellular ceramide rather than to CS extract. This approach allowed the study of specific responses to the sphingolipid, as CS contains more than 2,000 chemicals, and the precise dosing and exposure time in cell culture that mimics human exposure is not known. Furthermore, COPD is known to progress even after affected individuals stop smoking. For these reasons, the effect of chronic CS exposure was investigated by comparing primary cells isolated from individuals with a history of cigarette smoking to naive cells isolated from nonsmokers. To our knowledge, this is the first direct comparison of this kind.

We previously determined ceramide species in human acellular bronchoalveolar lavage as a window into the content of ceramide in lung environment. Although

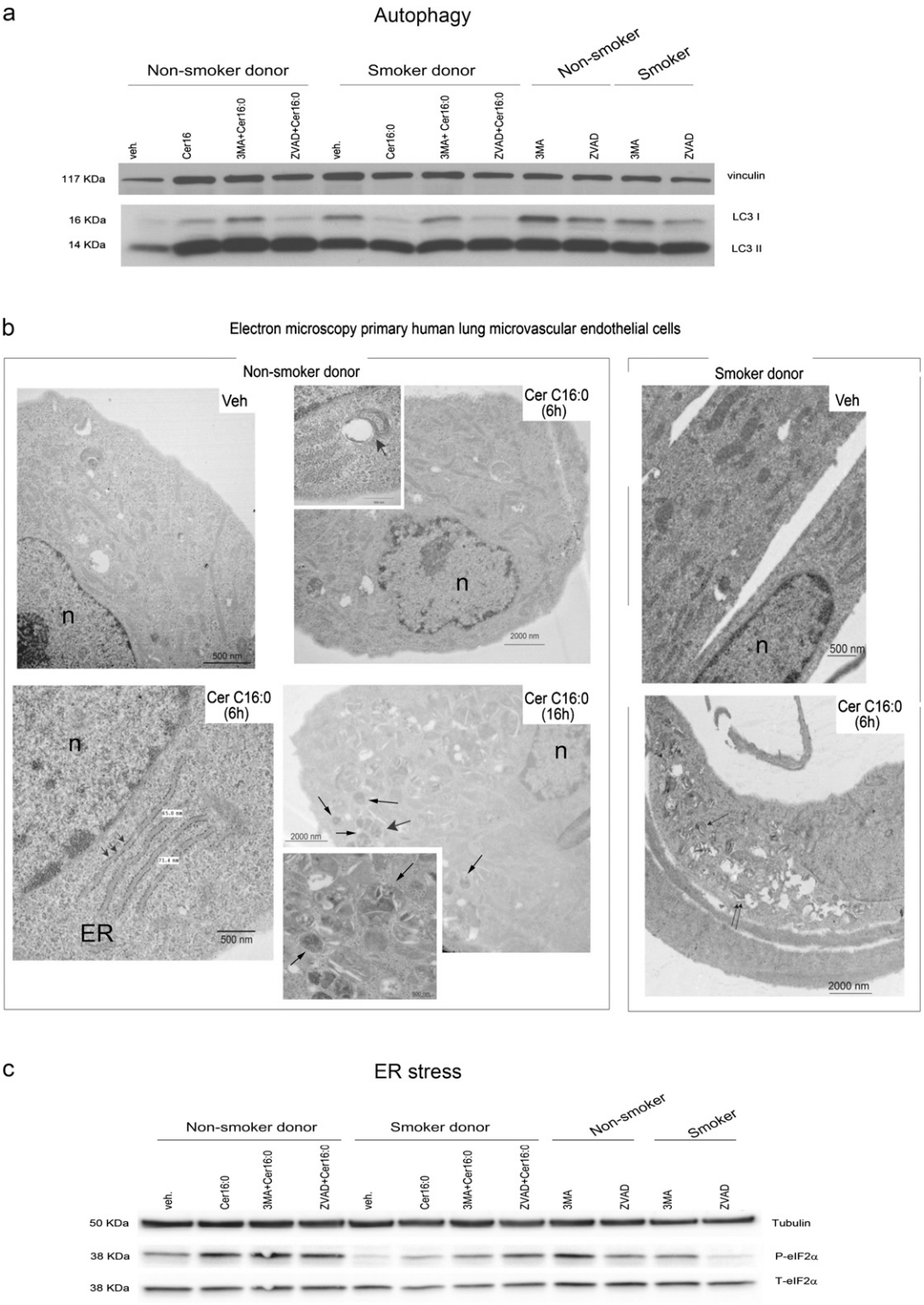

Figure 4. Autophagy and endoplasmic reticulum (ER) stress in human lung microvascular endothelial cells treated with Cer16. (*a*) Western blot of microtubule-associated protein-1 light-chain 3 (LC3) -I and LC3-II and vinculin (as loading control) in cells treated with Cer16 (10 μM, 16 h) or Veh, and effect of general caspase inhibitor, known commercially as ZVAD-fmk (0.1 mM, 1 h pretreatment) or autophagy inhibitor 3-MA (5 mM, 1 h pretreatment). (*b*) Representative electron microscopy images of cells after treatment with Cer16 or Veh for 6 or 16 hours. Noted are: nuclei (n), ER swelling (*arrowheads*, *lower panel*), autophagosomes (magnified in *lower panel inset*, *arrows*), and autophagosome–lysosome fusion (magnified in *upper panel inset*, *arrow*). (*c*) Western blot of phospho- and total eukaryotic translation initiation factor 2a (eIF2α) in cells similarly treated as in (*a*). Cells were treated with Cer16 or Veh control (PEG 2,000; 10 μM, 16 h) and pretreated with ZVAD-fmk (0.1 mM, 1 h) or 3-MA (5 mM, 1 h). β-tubulin was used as loading control.

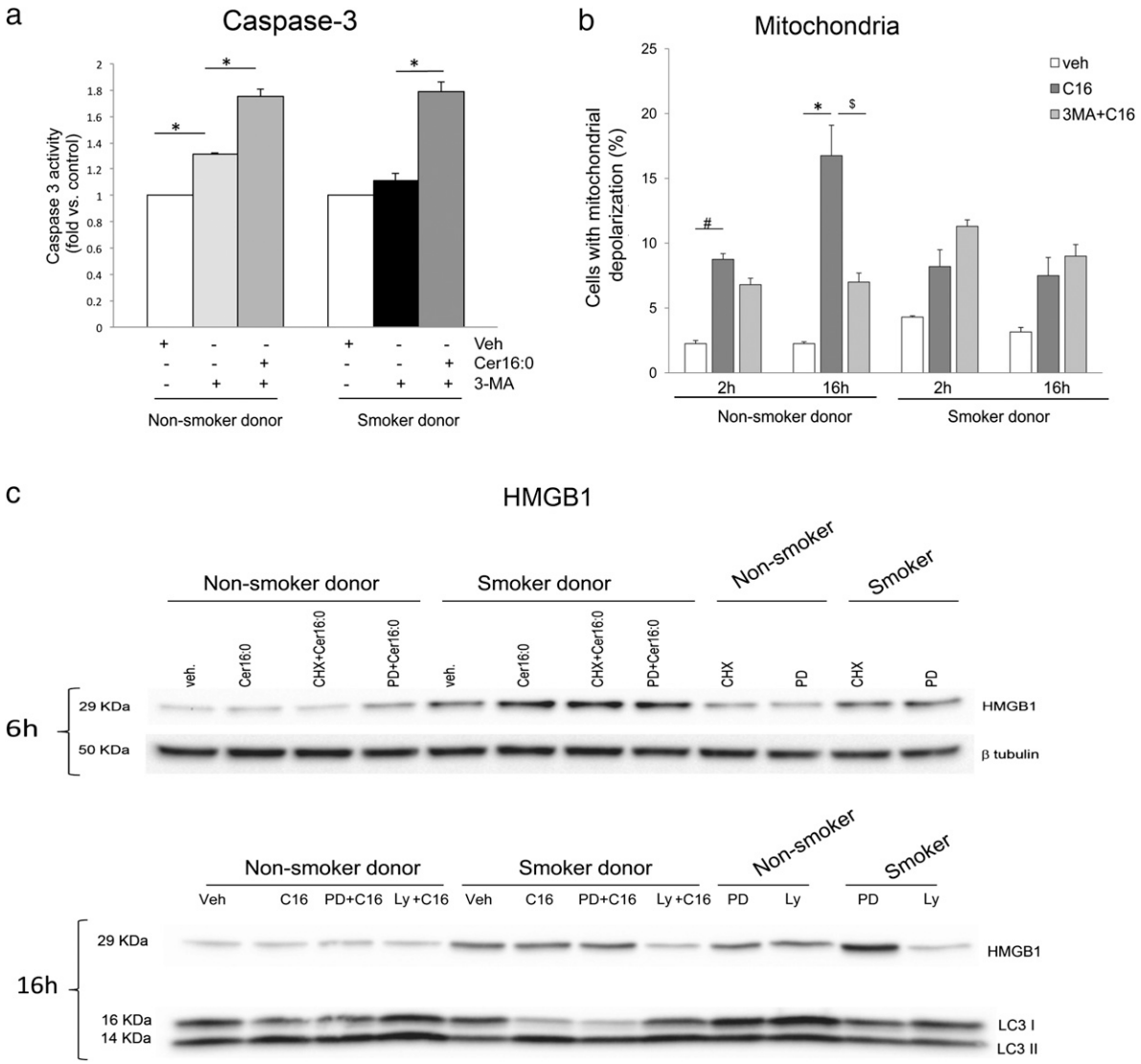

Figure 5. Autophagy and apoptosis interactions in human lung microvascular endothelial cells treated with Cer16. (*a* and *b*) Apoptosis measured by caspase-3 activity (*a*) or mitochondrial depolarization (*b*) in cells treated with Cer16 (10 μM; 2 hours in [*a*] and indicated time in [*b*]) or Veh, and effect of autophagy inhibitor, 3-MA (5 mM, 1 h pretreatment). Mean + SEM ($n = 4$, $^*P < 0.05$). (*c*). Levels of high-mobility group box 1 (HMGB1) or LC3-I and LC3-II measured by Western blot in cells treated with Cer16 (10 μM, for the indicated time) or Veh and either protein synthesis inhibitor, cycloheximide (CHX; 1 μg/ml, 1 h pretreatment), ERK1/2 inhibitor, PD98059 (PD; 50 μM, 1 h pretreatment), or Akt inhibitor LY294002 (LY; 30 μM, 1 h pretreatment).

the lung contains a vast range of ceramide species, one of the most abundant species is Cer16 (6). CS up-regulates Cer16 in the lung, and increasing Cer16 in the lungs of mice causes both endothelial and epithelial cell apoptosis *in vivo* (25). Primary human lung endothelial cells proved to be much more resistant to ceramide-induced cell death, associated with prompt induction of Akt signaling by ceramide. Furthermore, smoking potentially selected for a surviving cell population with higher proliferative capacity. This phenotype is reminiscent to that of endothelial cells isolated from patients with pulmonary arterial hypertension (PAH), where, after an initial apoptotic insult, there is selection of hyperproliferative and apoptosis-recalcitrant cells (26). Whereas typical plexiform lesions from idiopathic PAH are only rarely described in COPD, up to 70% of patients with COPD go on to develop PAH and pulmonary artery remodeling, features directly associated with worse prognosis and disease exacerbations (27). In addition, our results support findings *in vivo* of effects of smoking on pulmonary vasculature remodeling even in the absence of airspace destruction (28).

In lung cancer, $p16^{INK4a}$ is transcriptionally silenced through aberrant promoter hypermethylation due to cigarette smoking (29). It is possible that a similar mechanism occurs in endothelial cells exposed to chronic smoking, and may be responsible for the state of Akt and retinoblastoma protein hyperphosphorylation. The Akt signaling pathway was in large part responsible for endothelial cell fate, overall rendering the cells resistant to apoptosis induced by ceramides either directly or indirectly, during TNF-α and cycloheximide treatment (30). Despite resistance to

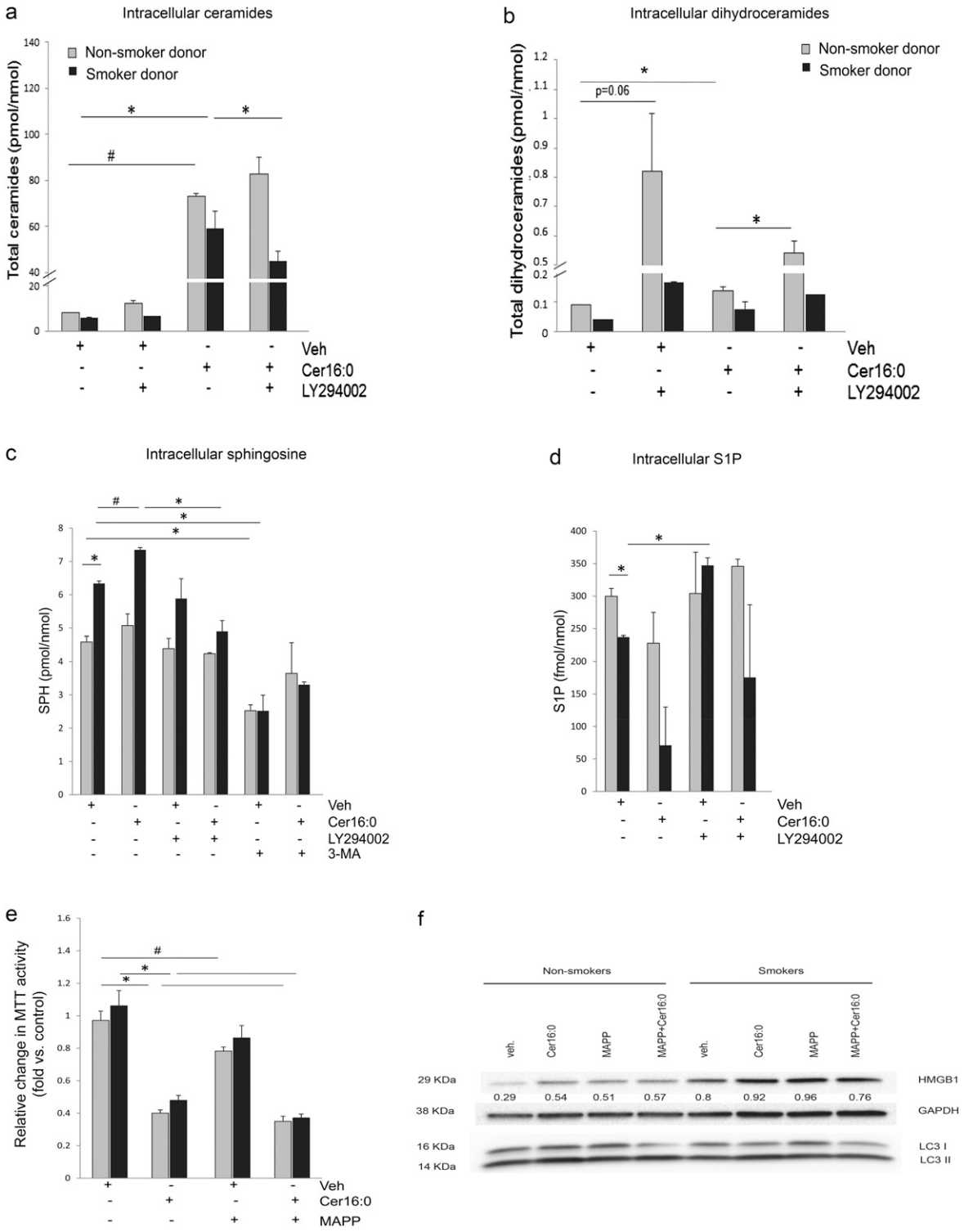

Figure 6. Modulation of intracellular sphingolipids by Cer16 in human lung microvascular endothelial cells. (*a–d*) Abundance of indicated sphingolipid species measured by combined liquid chromatography–tandem mass spectrometry in cells treated with Cer16 (10 μM, 2 h in [*a* and *b*]; 6 h in [*c* and *d*]) or Veh, and effect of Akt inhibitor LY294002 (30 μM, 1 h pretreatment) or autophagosome formation inhibitor, 3-MA (5 mM, 1 h pretreatment). Mean + SEM ($n = 2$; $^{*}P < 0.05$, $^{\#}P < 0.005$). (*e*) Cell metabolic activity assessed by MTT assay in cells treated with Cer16 (10 μM, 24 h) or Veh, and effect of ceramidase inhibitor, (1*S*,2*R*)-D-erythro-2-(*N*-myristoylamino)-1-phenyl-1-propanol (MAPP; 1 μM, 2 h pretreatment). Mean + SEM ($n = 3$; $^{*}P < 0.001$, $^{\#}P < 0.05$). (*f*) HMGB1, LC3-I, and LC3-II expression detected in protein lysate from cells treated with Cer16 (10 μM, 6 h) or Veh, and effect of MAPP. Glyceraldehyde 3-phosphate dehydrogenase (GAPDH) was used as loading control. Densitometry of HMGB1 expression normalized by loading control is indicated numerically in between blots. S1P, sphingosine 1-phosphate; SPH, sphingosine.

apoptosis, these cells displayed markedly decreased metabolic/proliferative rates, possibly via ceramide-induced regulation of cell cycle checkpoints. The significance to the pathogenesis of COPD and associated vascular abnormalities can only be speculated. It is possible that excessive apoptosis of vulnerable cells contributes to the typical alveolar wall destruction in emphysema. Because microvascular endothelial cells have been suggested to function as progenitor cells (31), and may therefore be involved in tissue repair, it is possible that the inhibitory effect of ceramide on their proliferative and metabolic activities is detrimental to tissue repair. On the other hand, exuberant proliferation of endothelial cells from smokers may lead to development of PAH in these lungs, and the inhibitory effect of ceramide on microvascular endothelial cell proliferation in this context may actually be beneficial. These scenarios remain to be answered in experimental models.

This study corroborates previous reports of increased ER stress in the setting of CS-induced emphysema (32), and highlights that endothelial cells also display this type of stress response to ceramide. Recent studies identified contributions of ceramides to ER stress and mitochondrial membrane potential alterations associated with apoptosis in insulin-secreting cells (33). In human lung endothelial cells, however, ceramide triggered ER stress together with prominent induction of autophagy, which, in turn, protected against further ER stress and minimized apoptosis. The mechanism by which ceramide induces autophagy and its full characterization in endothelial cells is not well described. Ceramide was shown to trigger homeostatic autophagy by decreasing nutrient transporter proteins, thus causing severe bioenergetic stress (34). In addition, both ER function (35) and autophagy (36, 37) can be controlled by various sphingolipid metabolites induced by ceramide. It is well established that exogenous (outside-in) ceramides activate endogenous sphingolipid production via *de novo* synthesis, which increases the production of the intermediate metabolite, DHC. Although much less abundant than ceramide, DHC itself can inhibit cell proliferation (15) and trigger autophagy. Our results suggest that DHC and SPH homeostasis might be regulated by Akt, and that cells respond to autophagy by further increasing SPH levels. Intracellular SPH did not trigger apoptosis; it rather appeared to be involved in autophagy and proliferative responses of cells exposed to ceramide.

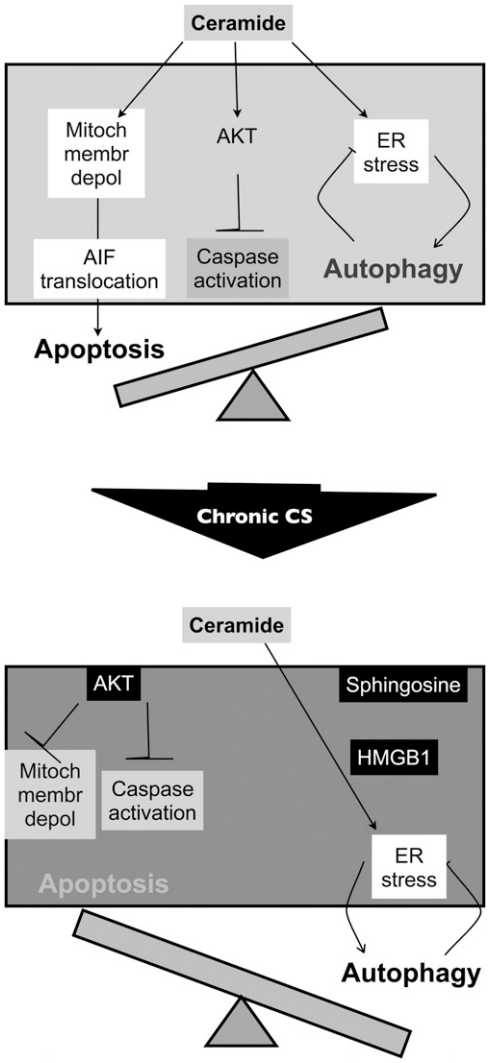

Figure 7. Schematic summarizing findings of Cer16 effect on human LMVECs isolated from nonsmokers compared with those isolated from smokers. Human naive LMVECs respond to ceramide by increasing ER stress and mitochondrial depolarization, which is associated with AIF-mediated, caspase-independent (Akt-inhibited caspases) apoptosis and autophagy (*top*). Chronic exposure to cigarette smoke (CS) is associated with Akt hyperphosphorylation and increased levels of SPH, which contributes to robust induction of autophagy associated with high HMGB1 levels, and which, together, contribute to develop an apoptotic-resistant phenotype (*bottom*).

Our work reveals a previously unappreciated link between ceramide, SPH, and HMGB1 in endothelial cell autophagy and apoptosis. In addition, knowing that HMGB1 conveys immunogenicity of the dying cell (38), the elevation of HMGB1 in lung endothelial cells challenged with ceramide may put forward the hypothesis that the ceramide–SPH–HMGB1 pathway participates in the autoimmune features of emphysema pathogenesis. Recent studies showed that HMGB1 promotes proliferation through Akt signaling pathway in hepatic stellate cells (39). Moreover, in mouse mesangial cells, HMGB1 increased the proliferation index, and the process was accompanied by down-regulation of $p16^{INK4a}$ (40). In turn, $p16^{INK4a}$ was demonstrated to be an efficient inhibitor of breast stromal fibroblasts proangiogenic effects through inhibition of Akt (41). Because LMVECs from smokers exhibit no $p16^{INK4a}$ accompanied by up-regulation of

HMGB1 and Akt hyperphosphorylation, we propose that the increased levels of SPH induced by chronic smoking may be related to Akt activation through HMGB1.

From a cell mass perspective, the decreased alveolar surface area in human emphysema lungs is the net results of an imbalance of alveolar structural cell apoptosis (excessive) and proliferation (7) (insufficient or ineffective). Murine *in vivo* models and cultured primary lung endothelial cells showed that ceramides activate executioner caspases-3/7 (2, 3, 14). In contrast, in naive primary human lung microvascular cells, palmitoyl-ceramide caused an unexpected immediate inhibition of caspase-3/7 activity, due to activation of autophagy and Akt. While in naive cells, the ceramide-induced Akt phosphorylation inhibited executioner caspases, but still allowed ceramide to induce apoptosis in a caspase-independent manner; the hyperphosphorylated Akt levels in cells from smokers inhibited ceramide-induced apoptosis altogether. Although solubilized palmitoyl-ceramide has been shown to induce a potent release of cytochrome *c* when added to mitochondrial suspensions (42) and ATP depletion followed by collapse of the inner mitochondrial membrane potential (43), the caspase-independent apoptosis via AIF translocation has not been previously appreciated in lung endothelial cells. Our data suggest that the baseline Akt hyperphoshorylation in cells from smokers contributes to a phenotype of resistance to proapoptotic insults, such as ceramide, including inhibition of caspase activation and that of mitochondria-related events that cause apoptosis. Although the "*de novo*" Akt phosphorylation induced by ceramide treatment in nonsmokers' cells is exerting similar anticaspase effects, it is not sufficient to inhibit mitochondria-related apoptosis. This suggests that mitochondrial tolerance to ceramide requires a different timing or context induced by the baseline Akt phosphorylation.

In conclusion, our study identifies exposure to CS as an important determinant of subsequent responses to stress, such as that induced by paracellular palmitoyl-ceramide. Human LMVECs respond to ceramide by potently up-regulating survival pathways, triggering ER stress, blocking cell proliferation, and inducing autophagy and caspase-independent AIF-mediated apoptosis, via a cross-talk among ERK1/2, Akt activation, and sphingolipid metabolite accumulation. Chronic exposure to CS changes the phenotype of these cells, selecting for a more proliferative population, with baseline alterations in $p16^{INK4a}$ expression, and Akt hyperphosphorylation, through yet-undetermined mechanisms. This phenotype renders cells from smokers less likely to die by apoptosis from palmitoyl-ceramide exposure, despite potent mitochondrial activation but perhaps due to robust induction of autophagy associated with high HMGB1 levels. This study prompts future *in vivo* investigations to determine the implication of these phenotypes to disease initiation and progression in the lungs of smokers, and to the development of pulmonary hypertension in this setting. Furthermore, our results indicate a complex cross-talk between ER stress, autophagy, and apoptosis, which is, in part, mediated by the intracellular changes in sphingolipid metabolites, and highlight the importance of the ceramide species- and disease-specific context for the ultimate fate of multi-input signaling pathways. ■

Author disclosures are available with the text of this article at www.atsjournals.org.

Acknowledgments: The authors acknowledge Natalia I. Rush, Patricia Smith, Dorothy K. Ndishabandi, Osato Ogbeifun, and Caroline Miller for expert technical assistance. They thank Tim Lahm, M.D., and Rubin M. Tuder, M.D., for helpful editing of the manuscript.

References

1. Tuder RM, Petrache I. Pathogenesis of chronic obstructive pulmonary disease. *J Clin Invest* 2012;122:2749–2755.
2. Petrache I, Natarajan V, Zhen L, Medler TR, Richter AT, Cho C, Hubbard WC, Berdyshev EV, Tuder RM. Ceramide upregulation causes pulmonary cell apoptosis and emphysema-like disease in mice. *Nat Med* 2005;11:491–498.
3. Petrache I, Medler TR, Richter AT, Kamocki K, Chukwueke U, Zhen L, Gu Y, Adamowicz J, Schweitzer KS, Hubbard WC, *et al*. Superoxide dismutase protects against apoptosis and alveolar enlargement induced by ceramide. *Am J Physiol Lung Cell Mol Physiol* 2008;295:L44–L53.
4. Bodas M, Min T, Vij N. Critical role of CFTR-dependent lipid rafts in cigarette smoke–induced lung epithelial injury. *Am J Physiol Lung Cell Mol Physiol* 2011;300:L811–L820.
5. Filosto S, Castillo S, Danielson A, Franzi L, Khan E, Kenyon N, Last J, Pinkerton K, Tuder R, Goldkorn T. Neutral sphingomyelinase 2: a novel target in cigarette smoke–induced apoptosis and lung injury. *Am J Respir Cell Mol Biol* 2011;44:350–360.
6. Petrusca DN, Gu Y, Adamowicz JJ, Rush NI, Hubbard WC, Smith PA, Berdyshev EV, Birukov KG, Lee CH, Tuder RM, *et al*. Sphingolipid-mediated inhibition of apoptotic cell clearance by alveolar macrophages. *J Biol Chem* 2010;285:40322–40332.
7. Yokohori N, Aoshiba K, Nagai A. Increased levels of cell death and proliferation in alveolar wall cells in patients with pulmonary emphysema. *Chest* 2004;125:626–632.
8. Hodge S, Hodge G, Holmes M, Reynolds PN. Increased airway epithelial and T-cell apoptosis in COPD remains despite smoking cessation. *Respir J* 2005;25:447–454.
9. Imai K, Mercer BA, Schulman LL, Sonett JR, D'Armiento JM. Correlation of lung surface area to apoptosis and proliferation in human emphysema. *Eur Respir J* 2005;25:250–258.
10. Chen ZH, Kim HP, Sciurba FC, Lee SJ, Feghali-Bostwick C, Stolz DB, Dhir R, Landreneau RJ, Schuchert MJ, Yousem SA, *et al*. EGR-1 regulates autophagy in cigarette smoke–induced chronic obstructive pulmonary disease. *PLoS ONE* 2008;3:e3316.
11. Deegan S, Saveljeva S, Gorman AM, Samali A. Stress-induced self-cannibalism: on the regulation of autophagy by endoplasmic reticulum stress. *Cell Mol Life Sci* 2013;70:2425–2441.
12. Tang D, Kang R, Livesey KM, Cheh CW, Farkas A, Loughran P, Hoppe G, Bianchi ME, Tracey KJ, Zeh HJ III, *et al*. Endogenous HMGB1 regulates autophagy. *J Cell Biol* 2010;190:881–892.
13. Petrache I, Kamocki K, Poirier C, Pewzner-Jung Y, Laviad EL, Schweitzer KS, Van Demark M, Justice MJ, Hubbard WC, Futerman AH, Ceramide synthases expression and role of ceramide synthase-2 in the lung: insight from human lung cells and mouse models. *PLoS ONE* 2013;8:e62968.
14. Medler TR, Petrusca DN, Lee PJ, Hubbard WC, Berdyshev EV, Skirball J, Kamocki K, Schuchman E, Tuder RM, Petrache I. Apoptotic sphingolipid signaling by ceramides in lung endothelial cells. *Am J Respir Cell Mol Biol* 2008;38:639–646.
15. Devlin CM, Lahm T, Hubbard WC, Van Demark M, Wang KC, Wu X, Bielawska A, Obeid LM, Ivan M, Petrache I. Dihydroceramide-based response to hypoxia. *J Biol Chem* 2011;286:38069–38078.
16. Schweitzer KS, Hatoum H, Brown MB, Gupta M, Justice MJ, Beteck B, Van Demark M, Gu Y, Presson RG Jr, Hubbard WC, *et al*. Mechanisms of lung endothelial barrier disruption induced by cigarette smoke: role of oxidative stress and ceramides. *Am J Physiol Lung Cell Mol Physiol* 2011;301:L836–L846.

17. Monick MM, Mallampalli RK, Bradford M, McCoy D, Gross TJ, Flaherty DM, Powers LS, Cameron K, Kelly S, Merrill AH Jr, *et al*. Cooperative prosurvival activity by ERK and Akt in human alveolar macrophages is dependent on high levels of acid ceramidase activity. *J Immunol* 2004;173:123–135.
18. Ferhani N, Letuve S, Kozhich A, Thibaudeau O, Grandsaigne M, Maret M, Dombret MC, Sims GP, Kolbeck R, Coyle AJ, *et al*. Expression of high-mobility group box 1 and of receptor for advanced glycation end products in chronic obstructive pulmonary disease. *Am J Respir Crit Care Med* 2010;181:917–927.
19. Hou C, Zhao H, Liu L, Li W, Zhou X, Lv Y, Shen X, Liang Z, Cai S, Zou F. High mobility group protein B1 (HMGB1) in asthma: comparison of patients with chronic obstructive pulmonary disease and healthy controls. *Mol Med* 2011;17:807–815.
20. Thorburn J, Frankel AE, Thorburn A. Regulation of HMGB1 release by autophagy. *Autophagy* 2009;5:247–249.
21. Kang R, Tang D, Schapiro NE, Livesey KM, Farkas A, Loughran P, Bierhaus A, Lotze MT, Zeh HJ. The receptor for advanced glycation end products (RAGE) sustains autophagy and limits apoptosis, promoting pancreatic tumor cell survival. *Cell Death Differ* 2010;17:666–676.
22. Livesey KM, Kang R, Vernon P, Buchser W, Loughran P, Watkins SC, Zhang L, Manfredi JJ, Zeh HJ III, Li L, Lotze MT, *et al*. p53/HMGB1 complexes regulate autophagy and apoptosis. *Cancer Res* 2012;72:1996–2005.
23. Wang W, Jiang H, Zhu H, Zhang H, Gong J, Zhang L, Ding Q. Overexpression of high mobility group box 1 and 2 is associated with the progression and angiogenesis of human bladder carcinoma. *Oncol Lett* 2013;5:884–888.
24. Sun KK, Ji C, Li X, Zhang L, Deng J, Zhong N, Wu XY, *et al*. Overexpression of high mobility group protein B1 correlates with the proliferation and metastasis of lung adenocarcinoma cells. *Mol Med Rep* 2013;7:1678–1682.
25. Kamocki K, Van Demark M, Fisher A, Rush NI, Presson RG Jr, Hubbard W, Berdyshev EV, Adamsky S, Feinstein E, Gandjeva A, *et al*. RTP801 is required for ceramide-induced cell-specific death in the murine lung. *Am J Respir Cell Mol Biol* 2013;48:87–93.
26. Masri FA, Xu W, Comhair SA, Asosingh K, Koo M, Vasanji A, Drazba J, Anand-Apte B, Erzurum SC. Hyperproliferative apoptosis-resistant endothelial cells in idiopathic pulmonary arterial hypertension. *Am J Physiol Lung Cell Mol Physiol* 2007;293:L548–L554.
27. Chaouat A, Bugnet AS, Kadaoui N, Schott R, Enache I, Ducoloné A, Ehrhart M, Kessler R, Weitzenblum E. Severe pulmonary hypertension and chronic obstructive pulmonary disease. *Am J Respir Crit Care Med* 2005;172:189–194.
28. Ferrer E, Peinado VI, Castañeda J, Prieto-Lloret J, Olea E, González-Martín MC, Vega-Agapito MV, Díez M, Domínguez-Fandos D, Obeso A, *et al*. Effects of cigarette smoke and hypoxia on pulmonary circulation in the guinea pig. *Eur Respir J* 2011;38:617–627.
29. Yanagawa N, Tamura G, Oizumi H, Shimazaki Y, Motoyama T. Frequent epigenetic silencing of the p16 gene in non–small cell lung cancers of tobacco smokers. *Jpn J Cancer Res* 2002;93:1107–1113.
30. Slowik MR, De Luca LG, Min W, Pober JS. Ceramide is not a signal for tumor necrosis factor–induced gene expression but does cause programmed cell death in human vascular endothelial cells. *Circ Res* 1996;79:736–747.
31. Alvarez DF, Huang L, King JA, ElZarrad MK, Yoder MC, Stevens T. Lung microvascular endothelium is enriched with progenitor cells that exhibit vasculogenic capacity. *Am J Physiol Lung Cell Mol Physiol* 2008;294:L419–L430.
32. Gan G, Hu R, Dai A, Tan S, Ouyang Q, Fu D, Jiang D. The role of endoplasmic reticulum stress in emphysema results from cigarette smoke exposure. *Cell Physiol Biochem* 2011; 28:725–732.
33. Lang F, Ullrich S, Gulbins E. Ceramide formation as a target in beta-cell survival and function. *Expert Opin Ther Targets* 2011;15:1061–1071.
34. Guenther GG, Peralta ER, Romero Rosales K, Yong SY, Siskind LJ, Edinger AL. Ceramide starves cells to death by downregulating nutrient transporter proteins. *Proc Natl Acad Sci USA* 2008;105: 17402–17407.
35. Lepine S, Allegood JC, Park M, Dent P, Milstien S, Spiegel S. Sphingosine-1-phosphate phosphohydrolase-1 regulates ER stress–induced autophagy. *Cell Death Differ* 2011;18:350–361.
36. Lavieu G, Scarlatti F, Sala G, Levade T, Ghidoni R, Botti J, Codogno P. Is autophagy the key mechanism by which the sphingolipid rheostat controls the cell fate decision? *Autophagy* 2007;3:45–47.
37. Ponnusamy S, Meyers-Needham M, Senkal CE, Saddoughi SA, Sentelle D, Selvam SP, Salas A, Ogretmen B. Sphingolipids and cancer: ceramide and sphingosine-1-phosphate in the regulation of cell death and drug resistance. *Future Oncol* 2010;6: 1603–1624.
38. Kepp O, Tesniere A, Schlemmer F, Michaud M, Senovilla L, Zitvogel L, Kroemer G. Immunogenic cell death modalities and their impact on cancer treatment. *Apoptosis* 2009;14:364–375.
39. Wang FP, Li L, Li J, Wang JY, Wang LY, Jiang W. High mobility group box-1 promotes the proliferation and migration of hepatic stellate cells via TLR4-dependent signal pathways of PI3K/Akt and JNK. *PLoS One* 2013;8:e64373.
40. Feng X, Hao J, Liu Q, Yang L, Lv X, Zhang Y, Xing L, Xu N, Liu S. HMGB1 mediates IFN-gamma–induced cell proliferation in MMC cells through regulation of cyclin D1/CDK4/p16 pathway. *J Cell Biochem* 2012;113:2009–2019.
41. Al-Ansari MM, Hendrayani SF, Tulbah A, Al-Tweigeri T, Shehata AI, Aboussekhra A. p16INK4A represses breast stromal fibroblasts migration/invasion and their VEGF-A–dependent promotion of angiogenesis through Akt inhibition. *Neoplasia* 2012;14:1269–1277.
42. Di Paola M, Cocco T, Lorusso M. Ceramide interaction with the respiratory chain of heart mitochondria. *Biochemistry* 2000;39: 6660–6668.
43. Ghafourifar P, Klein SD, Schucht O, Schenk U, Pruschy M, Rocha S, Richter C. Ceramide induces cytochrome c release from isolated mitochondria: importance of mitochondrial redox state. *J Biol Chem* 1999;274:6080–6084.